Maximizing detection and optimal characterization of local abnormal ventricular activity in nonischemic cardiomyopathy: LAVA$_{MAX}$ & LAVA$_{FLOW}$

Karl Magtibay, MASc,* Stéphane Massé, MASc,* Ahmed Niri, BSc,*
Robert D. Anderson, MBBS,* Ram B. Kumar, PhD,[†] D. Curtis Deno, MD, PhD,[†]
Kumaraswamy Nanthakumar, MD*

*From the *The Hull Family Cardiac Fibrillation Management Laboratory, Peter Munk Cardiac Centre, Toronto General Hospital, University Health Network, Toronto, Canada, and [†]Abbott Laboratories, St. Paul, Minnesota.*

BACKGROUND Sites of local abnormal ventricular activation (LAVA) are ventricular tachycardia (VT) ablation targets. In nonischemic cardiomyopathy (NICM), minute and sparse LAVA potentials are mapped with difficulty with direction-sensitive bipolar electrograms (EGM). A method for its optimal characterization independent of electrode orientation has not been explored.

OBJECTIVE Maximize voltages and calculate overall activation direction at LAVA sites, independent of catheter and wave direction, using omnipolar technology (OT) in NICM.

METHODS Four diseased isolated human hearts from NICM patients were mapped epicardially using a high-density grid. Bipolar EGMs with at least 2 activation segments separated by at least 25 ms were identified. We used OT to maximize voltages (LAVA$_{MAX}$) and measured overall wave direction (LAVA$_{FLOW}$) for both segments. Clinically relevant voltage proportion (CRVP) was used to estimate the proportion of directionally corrected bipoles. Concordance and changes in direction vectors were measured via mean vector length and angular change.

RESULTS OT provides maximal LAVA voltages (OT: 0.83 ± 0.09 mV vs Bi: 0.61 ± 0.06 mV, $P < .05$) compared to bipolar EGMs. OT optimizes LAVA voltages, with 32% (CRVP) of LAVA bipoles directionally corrected by OT. OT direction vectors at LAVA sites demonstrate general concordance, with an average of 62% ± 5%. A total of 72% of direction vectors change by more than 35° at LAVA sites.

CONCLUSION The omnipolar mapping approach allows maximizing voltage and determining the overall direction of wavefront activity at LAVA sites in NICM.

KEYWORDS Ablation; LAVA; Mapping; Omnipolar; Ventricular tachycardia

(Heart Rhythm O² 2021;2:529–536) © 2021 Heart Rhythm Society. Published by Elsevier Inc. This is an open access article under the CC BY-NC-ND license (http://creativecommons.org/licenses/by-nc-nd/4.0/).

Introduction

Local abnormal ventricular activity (LAVA) potentials are attractive targets for ventricular tachycardia (VT) ablation strategies.[1] Popularized by Jais and colleagues[2] in 2012, the histopathologic correlate of LAVA is thought to be surviving myocardial bundles poorly coupled to the rest of the scarred myocardium. Seminal work by de Bakker and Wittkampf[3] has previously demonstrated that LAVA tracts are formed from surviving bundles of fiber surrounded by inexcitable scar. However, in nonischemic cardiomyopathy (NICM), these LAVA potentials are known to be sparse.[4] In general, it is known that substrate ablation targets for VT in NICM are difficult to identify.[5] Though many have studied the effect of extrastimuli,[6,7] change in pacing site,[8,9] size of recording electrode,[10,11] interelectrode distance,[12,13] and linear vs grid mapping catheters[14,15] in improving detection of these targets, none have harvested the directional properties of LAVA and their distinct conduction properties to maximize their detection.

Omnipolar technology (OT)[16] has been used to characterize a local traveling wave (eg, wave direction, speed, and maximum voltage). OT has also been shown to alleviate the inherent directionality problem of bipolar electrograms (EGM). Thus, OT may provide a solution to the challenges posed by LAVA detection, namely (1) their directional sensitivity owing to minute voltage; (2) ability to determine overall conduction direction; and (3) deconstruction of signals containing LAVA activation into multiple distinct cardiac events. In this paper, we present a proof-of-concept for maximizing

Address reprint requests and correspondence: Dr Kumaraswamy Nanthakumar, Division of Cardiology, University Health Network, Toronto General Hospital, 150 Gerrard St W, GW3-526, Toronto, Ontario, Canada, M5G 2C4. E-mail address: kumar.nanthakumar@uhn.ca.

KEY FINDINGS

- The omnipolar methodology, a catheter orientation–independent and time activation–agnostic technique, could be used to analyze voltage fields at local abnormal ventricular activity (LAVA) sites of nonischemic cardiomyopathic hearts.

- The omnipolar methodology allows for independent maximization of individual voltage components of LAVA signals. This methodology could enable electrophysiologists to ensure detection and elimination of LAVA at the end of a catheter ablation procedure.

- Wave characteristics of individual components of LAVA potentials could be characterized from its voltage fields calculated with omnipolar methodology. In addition, this process could unmask conduction routes at LAVA sites that are otherwise undetectable with traditional bipolar mapping.

---

voltages (LAVA$_{MAX}$) and determining overall wave direction (LAVA$_{FLOW}$) for successive activations at a LAVA site (LAVA$_{FLOW}$).

Methods

LAVA EGMs with distinct multiple wave activations were identified from 4 diseased, isolated human hearts (IHH). The pathologies for each IHH are as follows: IHH1 (male, 58 years old): dilated cardiomyopathy; IHH2 (male, 38 years old): chemotherapy-induced cardiomyopathy; IHH3 (male, 64 years old): arrhythmogenic cardiomyopathy; IHH4 (female, 43 years old): postmyocarditis dilated cardiomyopathy. A wave activation was qualified as a signal segment with sharp potentials with at least 3–4 deflections.

Each heart was pace mapped using a custom high-density (HD) electrode array plaque stitched on the epicardium. The HD plaque consists of 112 electrodes (1 mm size) arranged in a 14 × 8 grid, equidistantly spaced by 2.4 mm between each electrode (Figure 1). Each heart was installed in a Langendorff setup perfused with Tyrode solution with flow rates maintained between 0.9 and 1.1 mL/g/min and a temperature of 37°C. Unipolar EGMs were simultaneously recorded using University Health Network's custom mapping system.[17,18] Informed consent was obtained from all donors, and IHH mapping protocols were approved by the University Health Network's research ethics board (Toronto, Ontario, Canada).

### Boundary between primary and LAVA bipolar wave activations

Figure 1 shows an example isochrone map of the primary activation from an IHH using the most negative slope detection. We show an example of fractionated bipolar EGMs, showing primary and LAVActivations, along 2 orthogonal axes: horizontal (Bi$_H$) and vertical (Bi$_V$) relative to our Langendorff suspension. For a simple case of 2 distinct activations within each bipolar EGM (Figure 2A), a marker is placed between the primary and LAVActivations if temporally separated by at least 25 ms. By empirical determination from all fractionated bipolar EGMs from all IHHs, 25 ms was a sufficient time separation to distinguish at least 2 activations. Out of 860 bipolar EGMs reviewed, 90 bipolar EGMs with at least 2 distinct activations were identified to be included for further processing and analysis.

Omnipolar electrograms: Voltage and direction

The derivation and explanation of the OT algorithm have been previously outlined by Deno and colleagues[16] and Massé and colleagues.[19] Using 3 closely spaced unipolar
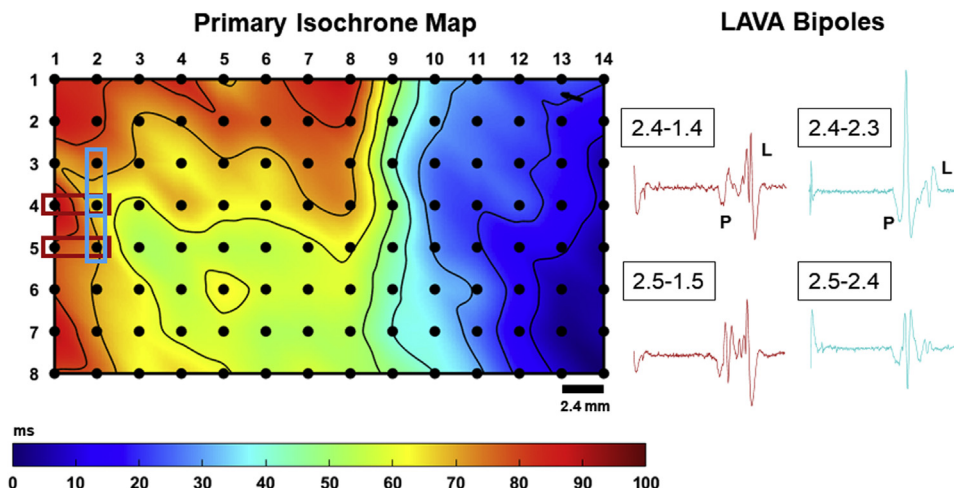
Figure 1   Ambiguity of local abnormal ventricular activity (LAVA) owing to bipolar electrogram directionality. **Left:** An isochrone map derived from the wave arrival times during pacing from an isolated human heart. **Right:** Bipolar electrograms, derived from 2 orientations—horizontal (red) and vertical (blue) showing their respective unipolar channels—show varying degrees of LAVA. Their column-row location indicates unipolar channels on the plaque, written as CX.RX. Owing to bipolar electrograms' directionality, LAVA could be seen from 2 different directions but with significantly different profiles within a small area. P indicates a primary activation, while L indicates a LAVActivation.
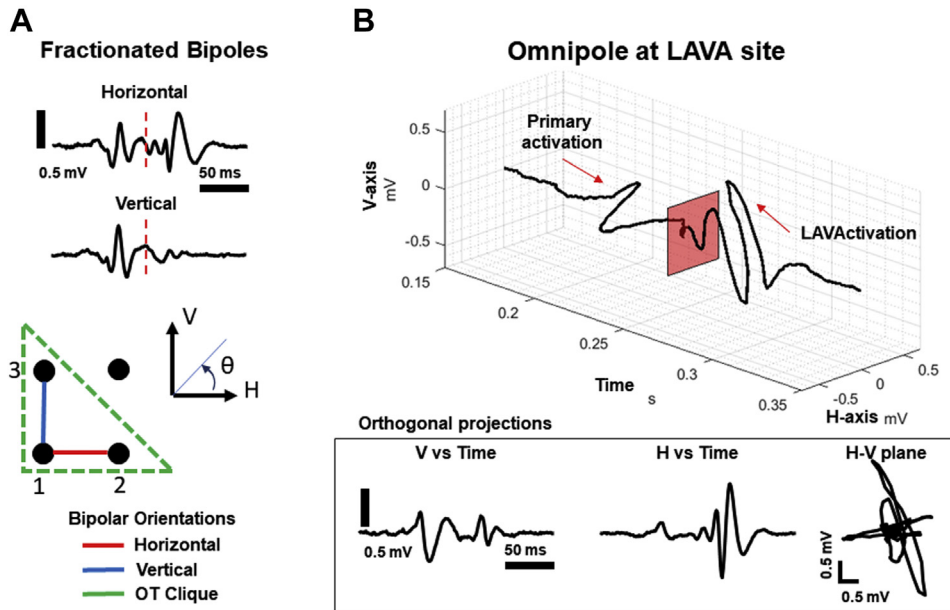
Figure 2   Temporal separation of local abnormal ventricular activity (LAVA) activations in bipolar and omnipolar electrograms. **A:** We show the temporal division of 2 activations within bipolar electrograms along 2 orientations from the same LAVA site. At the bottom, we show our bipolar orientations relative to our Langendorff suspension with a corresponding 2-dimensional (2D) plane and an angular reference. **B:** We also show the required minimum electrode configuration for 2D wavefronts and omnipolar technology (OT) processing. A time-stretched representation of a 2D voltage field represents a set of measurable bipolar electrograms within a LAVA site enclosed by 3 electrodes. On the H-time and V-time planes, orthogonal projections, relative to our high-density plaque, show examples of bipolar electrograms obtained from a 2D voltage field (H-V plane).

electrodes (right triangle clique; Figure 2A), a representation of a 2-dimensional (2D) voltage field of a traveling wave along the myocardial surface was calculated using OT, represented by 2 orthogonal bipolar EGMs, $V_x(t)$ and $V_y(t)$ projected at different angles, θ, such that

$$V_\theta(t) = \cos\theta \ \ V_x(t) + \sin\theta \cdot V_y(t).$$

Segments of maximized (and minimized) voltage peak-to-peak (V_{PP}) values for both primary ($PRI_{MAX/MIN}$) and LAVActivation ($LAVA_{MAX/MIN}$) segments were separately calculated from angular projections of $V_\theta(t)$. In addition, we calculated the overall activation direction, θ_{AD}, of a traveling wave, $\vec{a}_T$, based on the spatial and temporal characteristics of $V_\theta(t)$. Mathematical derivations of the parameters can be found in our Supplemental Material. Across IHHs, we calculated 162 $V_\theta(t)$'s from 3-electrode cliques. Only $V_\theta(t)$'s from cliques that shared unipolar electrodes with marked bipolar EGMs for both orthogonal directions (H & V) were included in the following quantitative analysis, decreasing our sample size to 55.

Quantitative analysis – Voltage and direction

Voltage analysis – LAVA_MAX
To test the differences and interactions between the V_{PP} values of $V_\theta(t)$'s segments and their bipole counterparts, we used a 2-way ANOVA and performed Bonferroni post-tests, both within a 95% confidence interval.

To test the directionality of primary and LAVActivation, we performed a simple comparison of voltage ratios, PRI_{MAX}/PRI_{MIN} and $LAVA_{MAX}/LAVA_{MIN}$, where a value other than 1 would indicate directionality. In addition, we performed a 1-sample, 1-tailed t test with a 95% confidence interval between the mean voltage ratios. Description of specificity and sensitivity study methods can be found in our Supplemental Material.

Lastly, we used clinically relevant voltage proportions (CRVP), similar to the version of the Clinical Benefit Proportion introduced by Deno and colleagues,[20,21] used in clinical cases to evaluate the proportion of bipolar V_{PP} values that PRI_{MAX} and $LAVA_{MAX}$ above certain thresholds directionally corrected. For example, a CRVP score of 0 means that PRI_{MAX} or $LAVA_{MAX}$ did not correct any corresponding bipolar V_{PP} values. Conversely, a score of 1 means that all of the corresponding bipolar V_{PP} values were corrected. We used 4 different thresholds, 0.5 mV, 0.4 mV, 0.3 mV, and 0.2 mV, to examine the performance of PRI_{MAX} and $LAVA_{MAX}$ under different ventricular substrate types.

Direction analysis – LAVA_FLOW
We further examined the directionality of OT vectors by measuring vector concordance within primary and LAVActivations among 4 OT unit vectors from nonoverlapping square areas of the HD plaque. We also examined OT vector concordance across primary and LAVActivations to highlight the difference of wave direction between activation types. Concordance was measured using OT vectors' angular deviation via mean vector length,[22] $\|\vec{a}_T\|$. A 1-sample, 1-tailed t test with a 95% confidence interval on mean vector
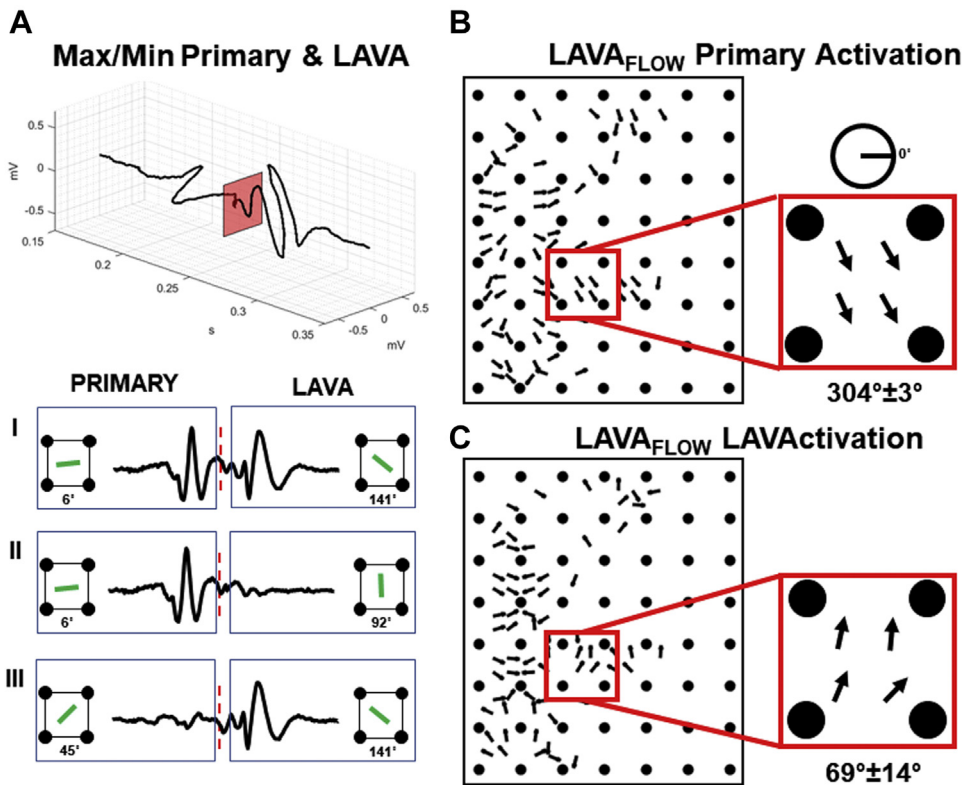
Figure 3 Maximized local abnormal ventricular activation (LAVA) omnipoles with $LAVA_{MAX}$ and tracking time evolution of activation direction at LAVA sites using $LAVA_{FLOW}$. **A:** The omnipolar methodology allows for reconfiguration of specific electrogram parts via maximization ($PRI_{MAX}/LAVA_{MAX}$) or minimization ($PRI_{MIN}/LAVA_{MIN}$) (I–IV) depending on mapping objectives. Three possible combinations of maximized (or minimized) omnipoles are shown: $PRI_{MAX}(t)+LAVA_{MAX}(t)$ (I), $PRI_{MAX}(t)+LAVA_{MIN}(t)$ (II), and $PRI_{MIN}(t)+LAVA_{MAX}(t)$ (III). Shown using green bars is the angle along which a portion of an omnipolar electrogram could be rotated to either maximize or minimize activations of interest. The omnipolar methodology (OT) also allows separate calculation of activation direction for **B:** primary and **C:** secondary activations at LAVA sites. OT allows tracking the time-evolution of activation direction vectors or the flow of electrical waves within a LAVA site ($LAVA_{FLOW}$). The general direction of OT vectors during a primary activation is significantly different compared to the vectors during a secondary activation. Blank grids indicate non-LAVA sites.

lengths was used to assess concordance within and between primary and LAVActivations.

Comparing the θ_{AD} between primary and LAVActivations, we used an empirically determined angular difference threshold in relation to OT vector coherence between primary and LAVActivations to suggest a significant change in OT vector angle. As in our observations from all IHH, a 95% OT vector coherence correspond to an angular difference of 35° (or ±17.5°) between $\theta_{AD,P}$ and $\theta_{AD,L}$. Using this strict threshold, we calculated the proportion of OT vectors that drastically change their direction from the primary to LAVActivation at LAVA sites across all IHHs.

Results
Omnipoles optimize LAVA detection
Omnipoles from a LAVA site were generated. The primary and LAVActivations could be configured depending on the activation segment of interest (ie, primary or LAVA). Figure 3A(I) illustrates maximized primary and LAVA segments, $[PRI_{MAX}(t) + LAVA_{MAX}(t)]$, at 2 different angular projections. We further show that a primary segment could

be minimized and maximize a LAVA segment, $[PRI_{MIN}(t) + LAVA_{MAX}(t)]$, shown in Figure 3A(III), or a primary segment maximized and minimize a LAVA segment, $[PRI_{MAX}(t) + LAVA_{MIN}(t)]$, shown in Figure 3A(II), with their corresponding angular projections.

Areas associated to LAVA sites for each IHH with respect to clique sizes (with percentage of the HD plaque) are as follows: IHH 1: 112 mm² (21%), IHH 2: 213 mm² (41%), IHH 3: 40 mm² (8%), and IHH 4: 101 mm² (19%). Shown in Figure 4A are the comparison of the average V_{PP} values for both bipolar and omnipolar EGMs (V_{PP} source) for 2 different activation types (primary and LAVActivation). $V_{PP}s$ from primary activation from any V_{PP} source are shown to be larger than the $V_{PP}s$ from LAVActivation: $Bi_{H,VPP}$: 1.17 ± 0.20 mV (P) vs 0.61 ± 0.06 mV (L), $Bi_{V,VPP}$: 1.07 ± 0.17 mV (P) vs 0.56 ± 0.07 mV (L), MIN_{OT}: 0.63 ± 0.09 mV (P) vs 0.21 ± 0.02 mV (L), and MAX_{OT}: 1.70 ± 0.23 mV (P) vs 0.83 ± 0.09 mV (L). In Figure 4B, we show further evidence of the general directional nature of both primary and LAVActivations as indicated by their voltage V_{PP} ratios, with LAVActivations showing larger mean voltages
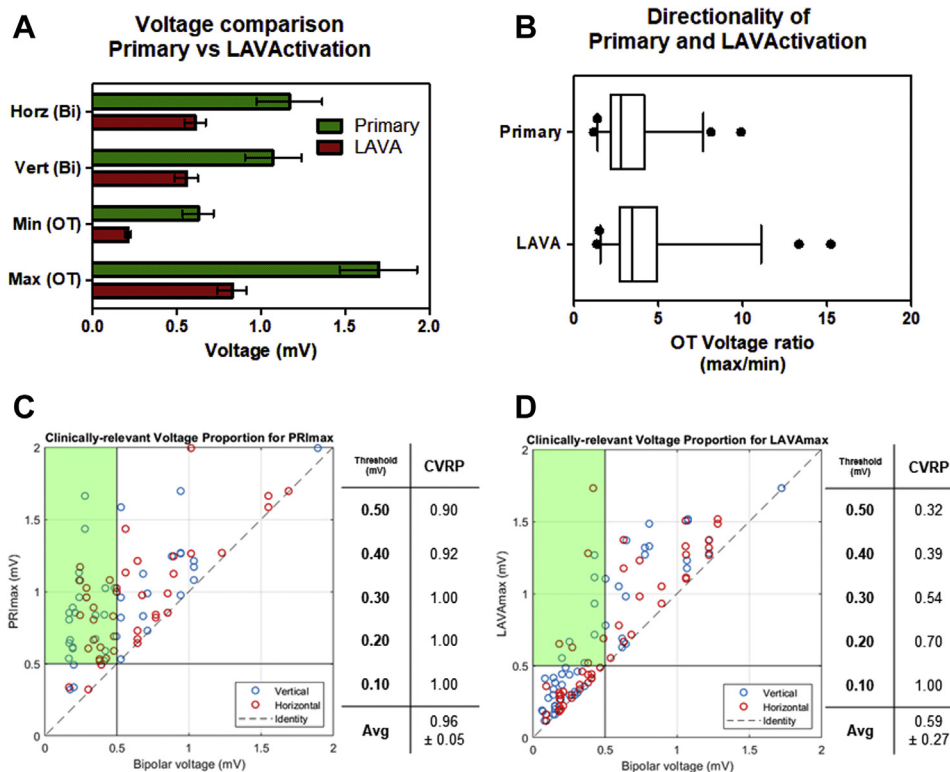
Figure 4   Voltage analysis of PRI$_{MAX/MIN}$ LAVA$_{MAX/MIN}$. **A:** Voltage comparison of voltage peak-to-peak values from different voltage sources (ie, horizontal bipole, minimum omnipole, etc) and activation types (ie, primary and LAVActivation). We show that omnipoles provide minimal and maximal peak-to-peak voltage values. **B:** Directionality of primary and LAVActivations is reflected from the distribution of their omnipolar technology (OT) voltage ratios (max/min) with the majority of ratios for both activation types greater than 1. We also show clinically relevant voltage proportions for **C:** PRI$_{MAX}$ and **D:** LAVA$_{MAX}$. For typical voltage thresholds, PRI$_{MAX}$ and LAVA$_{MAX}$ consistently provide larger voltage peak-to-peak values compared to bipoles.

ratios (4.20 ± 2.7, $P < .0001$) than primary activations (3.38 ± 0.25, $P < .0001$). Results of our sensitivity and specificity study can be found in our Supplemental Material.

LAVA$_{MAX}$ detection leads to better clinical recognition

Analysis of the CRVP values for PRI$_{MAX}$ shows that for a voltage threshold of 0.5 mV (representing border of fibrosed/scarred sites), 90% of bipolar V$_{PP}$ values are corrected for direction during the primary activation. In contrast, CRVP for LAVA$_{MAX}$ corrects 32% of bipolar V$_{PP}$ values during the LAVActivation. However, as the voltage threshold decreases, the proportion of directionally corrected bipolar V$_{PP}$ values increases for both primary and LAVActivations. PRI$_{MAX}$ and LAVA$_{MAX}$ reach perfect correction at 0.30 mV and 0.10 mV voltage thresholds, respectively, with average CRVP values across multiple voltage thresholds at 0.96 ± 0.05 for PRI$_{MAX}$ and 0.59 ± 0.27 for LAVA$_{MAX}$. A summary of our CRVP analysis is shown in Figure 4C and 4D.

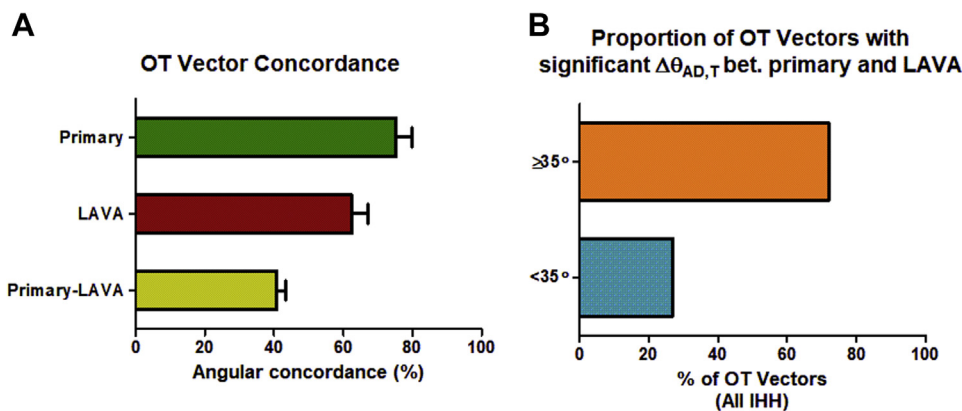## LAVA$_{FLOW}$: Omnipoles provide general wave directions of LAVA tracts

We show in Figure 3B and 3C unique OT vector fields generated for primary and LAVActivations, respectively. These

figures indicate the presence of 2 time-staggered electrical waves within a LAVA site. Highlighted in red are vectors as examples (Figure 3C).

Analysis of OT vector concordance within primary and LAVActivation segments show high averages, as indicated by high average mean vector lengths $75\% \pm 5\%$ and $62\% \pm 5\%$ ($P < .0001$), respectively, further suggesting directionality of both activation types. On the other hand, OT vector concordance between primary and LAVActivation segments shows only $41\% \pm 3\%$ ($P < .0001$) concordance, suggesting a difference of activation directions between the primary and LAVActivation. The summary of OT vector coherence analysis is shown in Figure 5A. Across all IHHs, analysis of proportions shows that 72% of OT vectors change direction by more than or equal to $35°$ ($\pm 17.5°$) between primary and LAVActivation, as shown in Figure 5B.

Discussion

The significant finding of our work is that LAVA potentials in NICM exhibit directionality, distinct from primary activation, and this finding has important clinical implications. The practical consequence is that the prevalence of LAVA may be underestimated on multielectrode mapping catheters unless a directional analysis is incorporated. Our findings also suggest that ablation catheter determination of elimination of LAVA is not complete until a mapping strategy that is not

A

OT Vector Concordance

Angular concordance (%)

B

Proportion of OT Vectors with significant $\Delta\theta_{AD,T}$ bet. primary and LAVA

% of OT Vectors
(All IHH)

Figure 5 Direction analysis of LAVA$_{FLOW}$. **A:** We further show the directionality of primary and local abnormal ventricular activation (LAVA) potentials through their omnipolar technology (OT) vector concordance. High vector concordance is shown from OT vectors for primary (green) and LAVActivations (red). Furthermore, low vector concordance between primary and LAVActivations (yellow) shows that waves travel in different directions for each activation type. **B:** To illustrate this, we show that 72% of OT vectors across all mapped isolated hearts change OT vector angle by more than or equal to 35°.

directionally dependent on these sites has been conducted. The detection of these potentials during grid mapping and lack thereof when mapping with ablation catheters could be addressed in the following manner: (1) 2-dimensional, voltage field methodology using orthogonal bipole voltage pairs can be used to delineate LAVA in an arrhythmogenic substrate; (2) directional correction using OT negates the effect of wavefront directionality and is independent of electrode orientation, optimizes detection (LAVA$_{MAX}$), and unmasks conduction routes (LAVA$_{FLOW}$).

In contemporary practice, there is an increasing reliance on substrate-based mapping, as most intraprocedural VT is noninducible or unmappable owing to hemodynamic instability.[23–25] Voltage mapping in sinus rhythm (or paced rhythm) identifies abnormal EGM and channels critical for reentrant circuits located within low voltage or scar. However, differences in the mapping catheter (electrode size, interelectrode spacing, and configuration) and activation wavefront adversely influence bipolar EGM components. Wavefront directionality not only affects substrate characterization but also unmasks critical isthmus anatomy[26] and border zone heterogeneity.[27] Multielectrode, high-density catheters have improved the mapping resolution of low-voltage regions by revealing surviving channels that may be missed using standard catheters.[28,29]

Bipolar directionality strongly impacts local voltage properties. Takigawa and colleagues[30] examined diagonally orthogonal bipolar pairs in an animal infarct model. They found an overall voltage variation of 0.28 mV (median of 30%) between orthogonal pairs, most pronounced in border zone scar. Directional variation and anisotropy accentuation in scar regions is a consistent finding, as shown by their voltage ratios, and is likely a consequence of architectural heterogeneity and functional conduction block. As such, limitations in traditional mapping methods may overlook critical LAVA potentials. We demonstrated that OT eliminates this directional error and maximizes LAVA detection by aligning the bipole to the activation

axis, which is evident through comparing their average LAVA$_{MAX}$ values across all IHHs. LAVA$_{MAX}$ presents 33% and 26% higher V$_{PP}$ values compared to its horizontal and vertical bipolar counterparts, respectively. A voltage threshold of 0.5 mV, typically associated with border zone scar, showed that 32% of LAVA sites could be better identified by LAVA$_{MAX}$ than traditional bipolar V$_{PP}$ values, as shown in our CRVP analysis. As the voltage threshold is lowered to 0.1 mV, the approximate voltage value from surviving tracts within fibrotic or scarred tissues, the proportion of LAVA sites identified increases by as much as 68%. Although these LAVA$_{MAX}$ values are small, they could still be identified from EGMs' noise envelope with some accuracy, as shown from our sensitivity analysis. A similar case is true for the directional influence on LAVA, since a fraction of these signals may be distinguishable from the noise envelope. The recognizability of LAVA potentials from the noise envelope becomes important when switching from multidirectional mapping grid electrode to ablation catheter with a unidirectional assessment of LAVAs.

Nonetheless, we show that OT could be used to generate either maximized or minimized segments of a fractionated EGM, independent of catheter orientation. As OT is independent of wavefront direction and electrode orientation, LAVA$_{MAX}$ may improve the identification of ventricular arrhythmogenic substrate and electroanatomical maps.[19,31] Furthermore, having information on multiple traveling waves at a LAVA site could be beneficial for independent analyses of related or decoupled cardiac electrophysiological events

Animation techniques such as flashing dot mapping pioneered by Downar and colleagues[32] and then followed by ripple mapping[33] have been previously used to characterize multiple events during arrhythmic episodes; however, they have been limited by the information collected either from traditional bipolar EGMs or by sensing catheter orientation. In this study, we extended OT's application into this domain

by processing EGMs with the assumption that more than 1 traveling wave exists within a brief time interval. Furthermore, we provided some evidence of its feasibility by introducing LAVA$_{FLOW}$. Using this OT extension, we showed that the traveling waves for primary and LAVActivations are distinct from each other, as indicated by the average vector nonconcordance of $102° \pm 61°$ between primary and LAVA activations.

Using a similar directional concept used in the current study, Nishimura and colleagues[34] have also demonstrated that developmental omnipolar software can visualize bipoles in different directions and maximize potentials at each site. We have expanded this concept by applying OT to track the source of the abnormal EGM and direction of activation. We anticipate that by using this methodology, the diastolic component of the VT circuit may be delineated while performing a sinus rhythm substrate map. The zone and direction of conduction in the surviving tracts can now be mapped, improving our understanding of the surviving tracts and their role in VT(s). This proof-of-concept study highlights the dynamic role of LAVA, being more than simply a static abnormal EGM. Translation of this concept, in an era where mapping system resolution improves and noise levels drop, controlling for different parameters (ie, pacing sites and rates) could lead to better detection of LAVAs and revelation of the role of LAVAs in arrhythmogenesis.

Limitations
We recognize some limitations of our study. We performed this study assuming that there are only 2 time-staggered traveling waves at a LAVA site while, as Downar and colleagues[32] previously showed, there could be more. In relation, a secondary isochrone map for LAVActivation was not included. As a result of our selection process, the number of qualified LAVA sites is so few that a dedicated isochrone map would not be as informative, since the selected LAVA sites were sparse and noncontiguous. Our process for identifying and separating LAVActivations is inherently subjective. It is an important limitation, as we are aware of complicated LAVA cases, such as prolonged LAVAs or LAVAs embedded within the primary activation. We also recognize that our study focuses on data acquired from the epicardial mapping of NICM with grid array catheters and may not be generalized to other locations. Histopathology of LAVA areas was not conducted owing to restrictions on human heart protocol. Therefore we could only give an approximate measure of LAVA areas in relation to OT cliques.

Conclusion
An omnipolar approach using a fixed-spaced electrode grid could maximize LAVA amplitudes and allow for independent analyses of activation directions. This approach may allow for better recognition of LAVA potentials in NICM compared to traditional bipolar mapping.

Appendix
Supplementary data
Supplementary data associated with this article can be found in the online version at https://doi.org/10.1016/j.hroo.2021.08.006.

References
1. Arenal A, Glez-Torrecilla E, Ortiz M, et al. Ablation of electrograms with an isolated, delayed component as treatment of unmappable monomorphic ventricular tachycardias in patients with structural heart disease. J Am Coll Cardiol 2003; 41:81–92.
2. Jais P, Maury P, Khairy P, et al. Elimination of local abnormal ventricular activities: a new end point for substrate modification in patients with scar-related ventricular tachycardia. Circulation 2012;125:2184–2196.
3. De Bakker JM, Wittkampf FH. The pathophysiologic basis of fractionated and complex electrograms and the impact of recording techniques on their detection and interpretation. Circ Arrhythm Electrophysiol 2010;3:204–213.
4. Bhaskaran A, Tung R, Stevenson WG, et al. Catheter ablation of VT in non-ischaemic cardiomyopathies: endocardial, epicardial, and intramural approaches. Heart Lung Circ 2019;28:84–101.
5. Nakahara S, Tung R, Ramirez RJ, et al. Characterization of the arrhythmogenic substrate in ischemic and non-ischemic cardiomyopathy. J Am Coll Cardiol 2010;55:2355–2365.
6. De Riva M, Naruse Y, Ebert M, et al. Targeting the hidden substrate unmasked by right ventricular extrastimulation improves ventricular tachycardia ablation outcome after myocardial infarction. JACC Clin Electrophysiol 2018;4:316–327.
7. Jackson N, Gizurarson S, Viswanathan K, et al. Decrement evoked potential mapping: basis of a mechanistic strategy for ventricular tachycardia ablation. Circ Arrhythm Electrophysiol 2015;8:1433–1442.
8. Bogun F, Good E, Reich S, et al. Isolated potentials during sinus rhythm and pace-mapping within scars as guides for ablation of post-infarction ventricular tachycardia. J Am Coll Cardiol 2006;47:2013–2019.
9. Sacher F, Lim HS, Derval N, et al. Substrate mapping and ablation for ventricular tachycardia: the LAVA approach. J Cardiovasc Electrophysiol 2015;26:464–471.

10. Glashan CA, Tofig BJ, Tao Q, et al. Multisize electrodes for substrate identification in ischemic cardiomyopathy: validation by integration of whole heart histology. JACC Clin Electrophysiol 2019;5:1130–1140.

11. Barkagan M, Sroubek J, Shapira-Daniels A, et al. A novel multi-electrode catheter for high-density ventricular mapping: electrogram characterization and utility for scar mapping. Europace 2020;22:440–449.

12. Tung R, Kim S, Yagishita D, et al. Scar voltage threshold determination using ex vivo magnetic resonance imaging integration in a porcine infarct model: influence of interelectrode distances and three-dimensional spatial effects of scar. Heart Rhythm 2016;13:1993–2002.

13. Takigawa M, Relan J, Kitamura T, et al. Impact of spacing and orientation on the scar threshold with a high-density grid catheter. Circ Arrhythm Electrophysiol 2019;12:e007158.

14. Jiang R, Beaser AD, Aziz Z, et al. High-density grid catheter for detailed mapping of sinus rhythm and scar-related ventricular tachycardia: comparison with a linear duodecapolar catheter. JACC Clin Electrophysiol 2020; 6:311–323.

15. Proietti R, Adlan AM, Dowd R, et al. Enhanced ventricular tachycardia substrate resolution with a novel omnipolar high-density mapping catheter: the omnimapping study. J Interv Card Electrophysiol 2020;58:355–362.

16. Deno DC, Balachandaran R, Morgan D, et al. Orientation independent catheter-based characterization of myocardial activation. IEEE Trans Biomed Eng 2017; 64:1067–1077.

17. Massé S, Sevaptisidis E, Parson ID, et al. A data acquisition system for real-time activation detection of cardiac electrograms I: hardware. Conf Proc IEEE Eng Med Biol Soc 1991;13:0780–0781.

18. Massé S, Sevaptisidis E, Parson ID, et al. A data acquisition system for real-time activation detection of cardiac electrograms II: software. Conf Proc IEEE Eng Med Biol Soc 1991;13:782–783.

19. Massé S, Magtibay K, Jackson N, et al. Resolving myocardial activation with novel omnipolar electrograms. Circ Arrhythm Electrophysiol 2016;9:e00410.

20. Deno DC, Lee VG, Davis EK, et al. Quantifying bipolar bias in atria and guidance to map physiologically relevant low-voltage [abstract]. Heart Rhythm 2020; 17:S197–S198.

21. Massé S, Magtibay K, Niri A, et al. A more definitive method to map arrhythmogenic substrate for VT ablation [abstract]. Heart Rhythm 2020;17:S606.

22. Berens P. CircStat: a MATLAB toolbox for circular statistics. J Stat Softw 2009; 31:1–21.

23. Tung R, Vaseghi M, Frankel DS, et al. Freedom from recurrent ventricular tachycardia after catheter ablation is associated with improved survival in patients with structural heart disease: an international VT ablation center collaborative group study. Heart Rhythm 2015;12:1997–2007.

24. Di Biase L, Santangeli P, Burkhardt DJ, et al. Endo-epicardial homogenization of the scar versus limited substrate ablation for the treatment of electrical storms in patients with ischemic cardiomyopathy. JACC 2012; 60(2):132–141.

25. Di Biase L, Burkhardt DJ, Lakireddy D, et al. Ablation of stable VTs versus substrate ablation in ischemic cardiomyopathy: the VISTA randomized multicenter trial. J Am Coll Cardiol 2015;66:2872–2882.

26. Martin CA, Martin R, Maury P, et al. Effect of activation wavefront on electrogram characteristics during ventricular tachycardia. Circ Arrhythm Electrophysiol 2019;12:e007293.

27. Rutherford SL, Trew ML, Sands GB, et al. High-resolution 3-dimensional reconstruction of the infarct border zone: impact of structural remodeling on electrical activation. Circ Res 2012;111:301–311.

28. Tschabrunn CM, Roujol S, Dorman NC, et al. High-resolution mapping of ventricular scar: comparison between single and multi-electrode catheters. Circ Arrhythm Electrophysiol 2016;9:e003841.

29. Berte B, Relan J, Sacher F, et al. Impact of electrode type on mapping of scar-related VT. J Cardiovasc Electrophysiol 2015;26:1213–1223.

30. Takigawa M, Relan J, Martin R, et al. Effect of bipolar electrode orientation on local electrogram properties. Heart Rhythm 2018;15:1853–1861.

31. Porta-Sánchez A, Magtibay K, Nayyar S, et al. Omnipolarity applied to equi-spaced electrode array for ventricular tachycardia substrate mapping. Europace 2019;21:813–821.

32. Downar E, Saito J, Colin Doig J, et al. Endocardial mapping of ventricular tachycardia in the intact human ventricle. III. Evidence of multiuse reentry with spontaneous and induced block in portions of re-entrant path complex. J Am Coll Cardiol 1995;25:1591–1600.

33. Linton NW, Koa-Wing M, Francis DP, et al. Cardiac ripple mapping: a novel three-dimensional visualization method for use with electroanatomic mapping of cardiac arrhythmias. Heart Rhythm 2009;6:1754–1762.

34. Nishimura T, Shatz N, Raiman M, et al. Optimization of near-field electrogram components for mapping of scar related ventricular tachycardia substrate: electrogram "tuning" with omnipolar mapping technology [abstract]. Heart Rhythm 2020;17:S569.